

Hot Tensile Properties of Filler Added Constant Current Gas Tungsten Arc Welded AISI 304HCu Super Austenitic Stainless Steel Joints

M. Vinoth Kumar, V. Balasubramanian, and A. Gourav Rao

¹ Research Scholar, ²Professor, Department of Manufacturing Engineering, Annamalai University, Annamalai Nagar, Tamil Nadu, India - 608002.

³Scientist, Naval Material Research Laboratory (NMRL), Ambarnath, Mumbai, India - 421506.

*Corresponding Author Email: Vinothmecho@gmail.com

ABSTRACT

AISI 304HCu austenitic stainless steel containing 2.3 to 3 (% wt) of Cu is mainly used in superheaters and reheater of ultra super critical (USC) boilers which operates over 600°C of steam temperature. Austenitic stainless steels welded by gas tungsten arc welding (GTAW) alters the phase composition, and microstructure of the steel in the fusion zone of welds and may affect the mechanical properties. In our previous investigation, it is found that autogenous welding of AISI 304HCu tubes resulted in segregation of alloying elements in the weld metal and resulted in joints with inferior tensile strength. Hence, in this study the high temperature tensile properties of filler added GTA welded AISI 304HCu tube joints were evaluated and correlated with the microstructural features. The tensile strength of the filler added GTA weld joints was higher than the parent metal at all test temperatures and the weld joint with filler addition was recommended for application in USC boilers.

Keywords: AISI 304HCu; gas tungsten arc welding; high temperature tensile properties; ultra super critical boilers.

1.0 INTRODUCTION

Ultra supercritical (USC) fossil power plants are under development worldwide to improve efficiency and reduce CO₂ emissions [1]. The efficiency of the power plant strongly depends on the steam temperature and pressure. The ultra super critical boilers operate at a steam pressure of about 300 bar and temperature of over 600°C. With the steam parameters continually to be increased, the first attempt to develop high efficiency ultra super critical steam generator has failed mainly due to the broke down in superheater and reheater tubes [2]. Hence, material development and selection are critical to the success of these efforts. Austenitic stainless steels are the most suitable materials for high temperature components where corrosion resistance is of importance in the ultra super critical boilers.

The recently developed AISI 304HCu austenitic stainless steel tubes containing 2.3 to 3 (% wt) of copper (Cu) is mainly used in superheaters and reheaters of ultra super critical boilers. AISI 304HCu belongs to 18%Cr-9%Ni system with additions of Cu, Niobium (Nb), and Nitrogen (N) for precipitation strengthening. Cu addition is the distinct addition to this stainless steel in comparison to the others. In addition to the oxidation resistance, Cu added to this steel precipitates as fine Cu rich phase during creep conditions and results in increased creep strength [3]. In addition to the oxidation resistance, Cu added to this steel precipitates as fine Cu rich phase during creep conditions and results in increased creep strength [3]. Production of these ultra super critical boilers requires lot of welding operations and gas tungsten arc welding (GTAW) is the mostly used welding process in fabrication of boilers.

In general, austenitic stainless steels welded by GTAW alter the phase composition, and microstructure of the steel such as producing coarse columnar grains in the fusion zone of welds. Such alteration in composition and microstructure can affect the high temperature tensile behaviour of the weld joint in contrast to the parent material behavior. In our previous investigation [4], it is found that autogenous welding of AISI 304HCu tubes resulted in segregation of alloying elements in the weld metal and yielded joints with inferior tensile strength than that of parent metal. From literature survey [5-7], it is found that the available literature on high temperature tensile properties of filler added GTA welded joints of AISI 304HCu stainless steel is very scant. Hence, in this study high temperature tensile properties of filler added GTA welded AISI 304HCu tube joints were evaluated and correlated with the microstructural features.

2.0 EXPERIMENTAL DETAILS

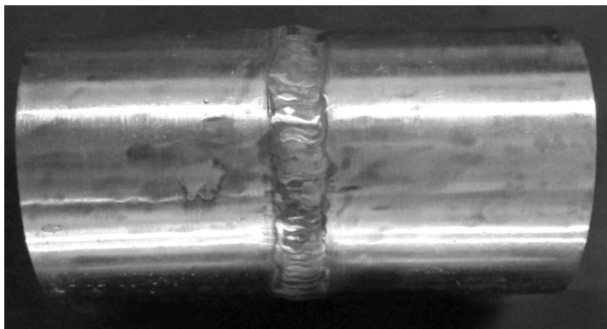
AISI 304HCu austenitic stainless steel tubes of outer diameter 57.1 mm and wall thickness of 3.5 mm were used in this investigation. The chemical composition of the parent metal in as-received condition and filler metal are given in **Table 1**.

The joints with single 'v' butt edge preparation were welded using GTAW process with filler wire. Argon was used as the shielding and purging gas with flow rate of 12 and 10 liters per minute respectively to prevent oxidation of the weld. The welding parameters used in this investigation are presented in **Table 2**.

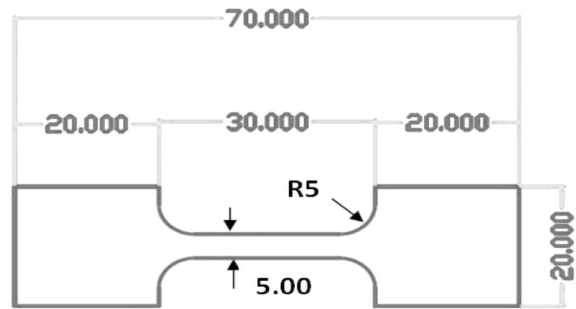
The photograph of weld joint in as-welded condition is shown **Fig. 1a**. The joints were inspected for visual defects and the specimens were extracted from the weld joints using wire-cut

Table 1 : Chemical composition (wt%) of Parent Metal (PM) and Filler Metal (FM)

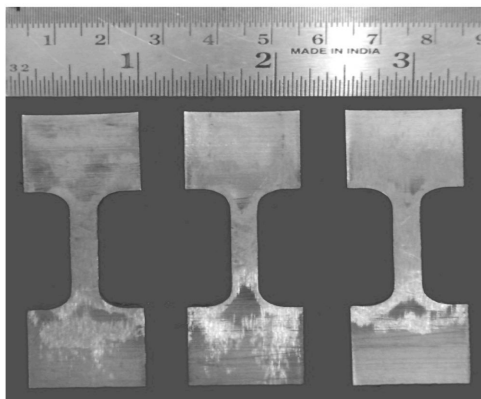
	C	Si	Mn	P	S	Cr	Ni	N	B	Cu	Nb	Mo
PM	0.086	0.23	0.81	0.021	0.0003	18.18	9.06	0.095	0.0039	3.080	0.045	-
FM	0.1	0.3	3.3	<0.01	<0.01	18.3	15.7	0.16	-	2.9	0.5	0.7



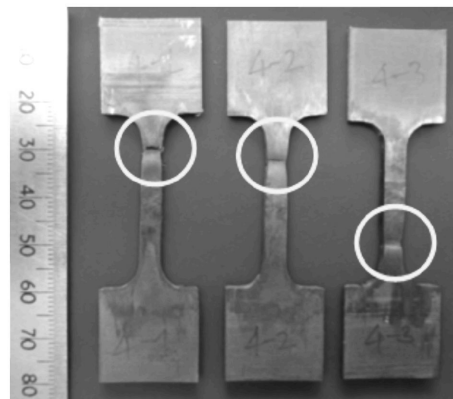
a. As welded tube joint



b. Dimensions of hot tensile specimen (mm)



c. Tensile specimen before test



d. Tensile specimen after test

Fig. 1 : Photograph of welded tubes and tensile specimen

Table 2 : Parameters for GTAW welding of AISI 304HCu

Power source type	Constant Current
Current (A)	75
Voltage (V)	11.3
Welding speed (mm/min)	75
Heat input (kJ/mm)	0.68

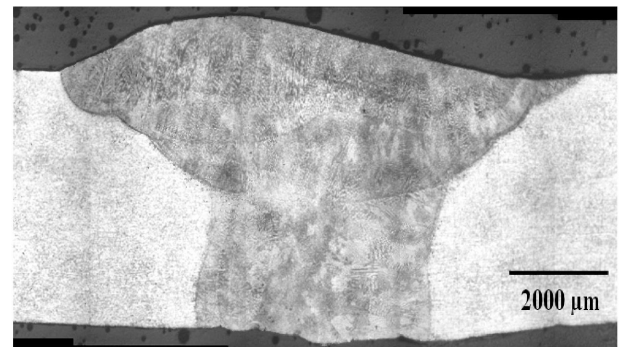
electric discharge machining. The schematic representation of hot tensile specimen dimensions was shown in **Fig. 1b**.

Tensile tests were carried out using an Instron universal testing machine (UTM) under the constant crosshead speed mode for a nominal strain rate of 1×10^{-3} S⁻¹ at test temperatures of room temperature (RT), 550°, 600° and 650° C. The UTM system was equipped with a three-zone resistance heating furnace and a computer with data acquisition system for obtaining digital load-elongation data. The photograph of hot tensile specimens before and after test was shown in **Fig. 1c** and **Fig. 1d** respectively. The specimen for microstructural examination were prepared using standard metallographic techniques and etched with 3 parts HCL and 1 part HNO for 5-10 s to reveal the microstructural features. The microstructural examination of the weld joint was carried out using light optical microscope (OM) and scanning electron microscopy (SEM). The hardness was measured across the weld, along the mid-thickness region using Vickers micro-hardness tester with a load of 500 g and dwell time of 15 s. The fracture surfaces of the tensile specimens were analysed using SEM to reveal the mode of fracture.

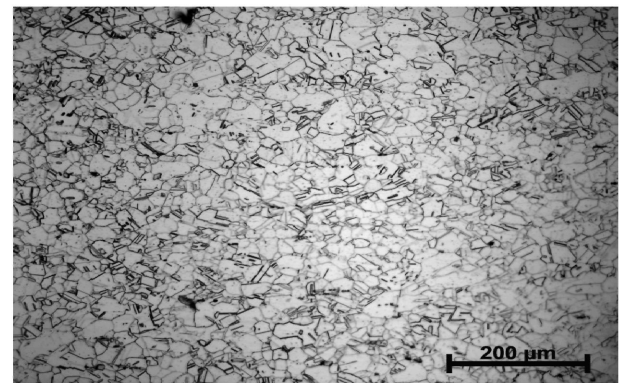
3.0 RESULTS

3.1 Microstructure

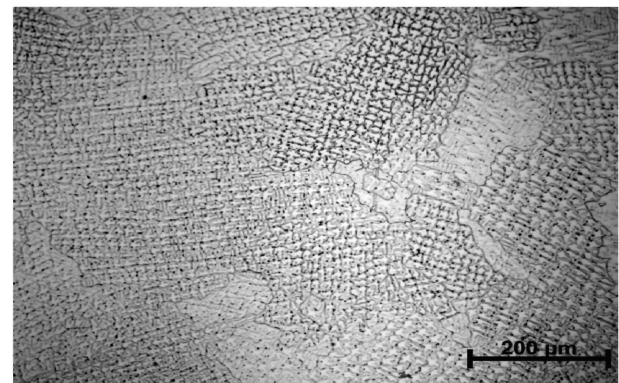
The microstructure of the as-received AISI 304HCu parent metal is shown in **Fig. 2a**. It consists of equiaxed austenitic grains of size 40-50 μm in annealed condition. The macrograph of the weld joint is shown in **Fig. 2b**, which shows complete fusion of the joint with absence of macro level defects. The **Fig. 2c** shows the weld metal microstructure which consists of equiaxed dendritic primary austenitic grains. The **Fig. 2d** shows the microstructure of the fusion line of the weld which consists of columnar austenitic grains which are preferentially oriented towards the weld centre, which is evident for the epitaxial grain growth occurred in this region. The heat affected zone consists of coarse grains than the unaffected parent metal.



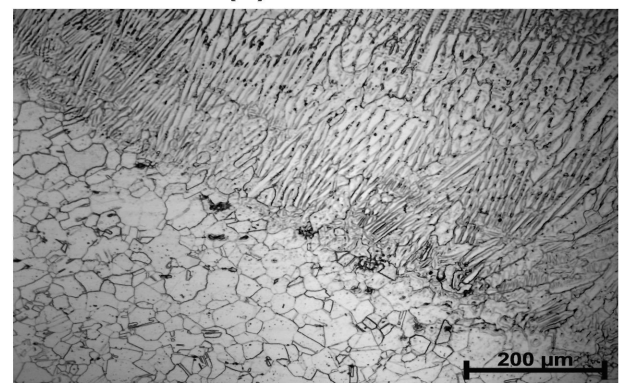
(a) Macrograph



(b) Parent metal



(c) Weld metal



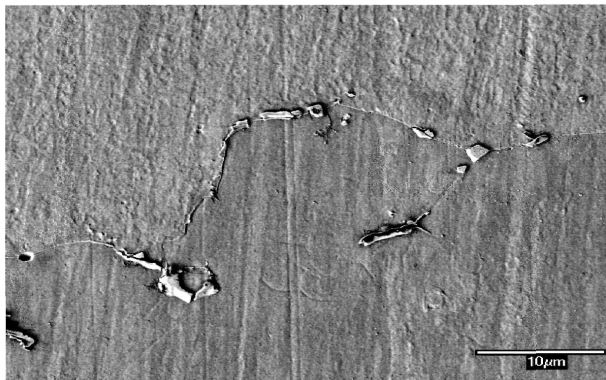
(d) Fusion line and HAZ

Fig. 2 : Optical micrographs of GTAW joint

The SEM micrograph of the weld metal is shown in **Fig. 3a** which reveals the presence of fully austenitic weld metal with no delta ferrite. The magnified SEM image of the weld metal shown in **Fig. 3b** reveals the presence of carbides along the grain boundary. The carbide marked by arrow was identified as (Mo,Nb) (C,N) by EDS analysis.



(a) Weld metal



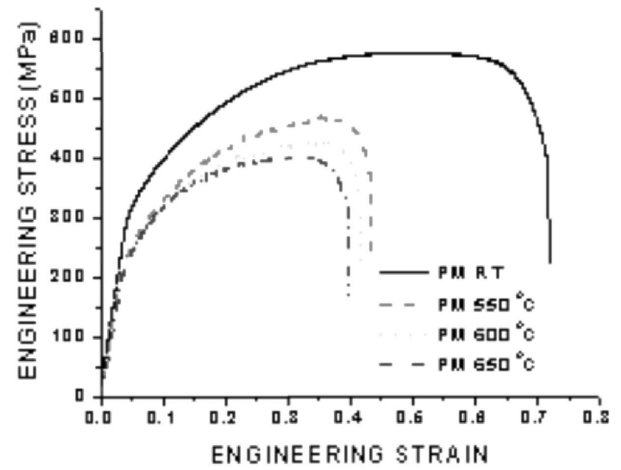
(b) Weld metal at Higher Magnification

Fig. 3 : SEM micrographs of GTAW joint

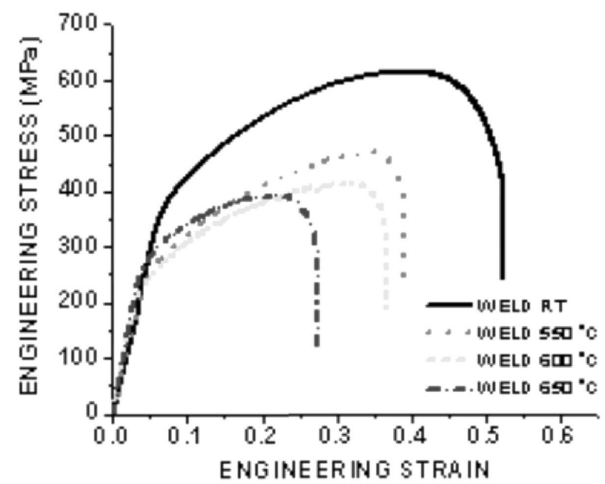
3.2 Tensile Properties

The engineering stress strain curves of parent metal and GTAW joint at various test temperatures are shown in **Fig. 4** and the values are presented in **Table 3**. The RT tensile strength of the weld joint (614.6 MPa) is 6.7 % higher than the parent metal tensile strength. The yield strength of the weld joint is 18.7 % higher than the parent metal. The elongation of the weld joint is 27.1 % lower than the parent metal elongation of 71.8 %. The weld joint exhibited joint efficiency of 106.7 % with failure in the parent metal.

The tensile strength of both parent metal and weld joint decreases with increase in test temperature. The tensile strength decreases by 30 % and 36 % for parent metal and weld joint respectively with increase in test temperature from RT to 650 °C. The elongation of the parent metal and weld joint



(a) Parent metal



(b) Weld joint

Fig. 4 : Engineering Stress - Strain curves at various test temperatures

decreases by 32 % and 25 % respectively with increase in temperature from RT to 650 °C, however the decrease in elongation for parent metal and weld joint in temperature range of 550 °C to 650 °C was minimum (refer **Table 3**).

3.3 Hardness

The micro hardness measured across the weld, along the mid thickness region was presented in **Fig. 5**. The weld metal has the highest hardness value in the joint with variations in hardness values within the region. The lowest hardness across the joint was recorded in the weld metal close to the fusion line. The HAZ region has not undergone softening due to welding and retained its hardness equivalent to that of the parent metal hardness value of 175 HV.

	Test temperature °C	0.2% Yield strength in Mpa	Ultimate tensile strength in Mpa	Elongation (%) (%)	Joint efficiency (%)
PM	RT	284.2	575.8	71.8	-
	550	205.5	465.8	43.0	-
	600	193.0	431.8	41.7	-
	650	204.3	401.8	39.6	-
GTAW joint	RT	349.6	614.6	52.3	106.7
	550	247.3	470.2	39.2	101.0
	600	196.3	413.6	36.6	95.8
	650	240.8	392.7	27.3	97.7

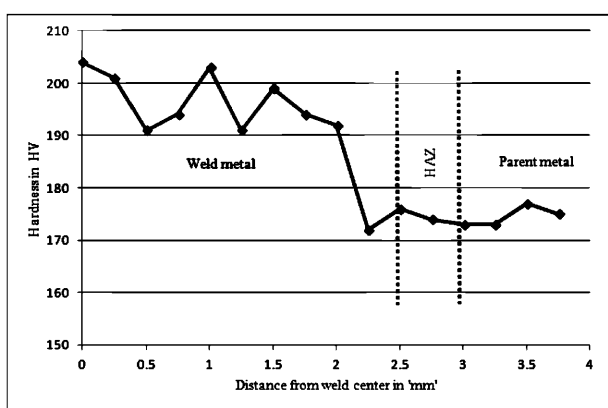


Fig. 5 : Hardness profile across the weld center line of GTAW joint

3.4 Fracture Surfaces

The SEM fractographs of tensile specimen are shown in Fig. 6. The Fig. 6a and Fig. 6b represents the fracture surface of parent metal and weld joint tested at room temperature respectively. In both cases the fracture has occurred in the parent metal. The fracture was considered to be ductile fracture with fine dimples around the voids, which are associated with the precipitates present in the austenitic matrix. The Fig. 6c and Fig. 6d shows the fracture surface of the parent metal and weld joint tested at 600 °C.

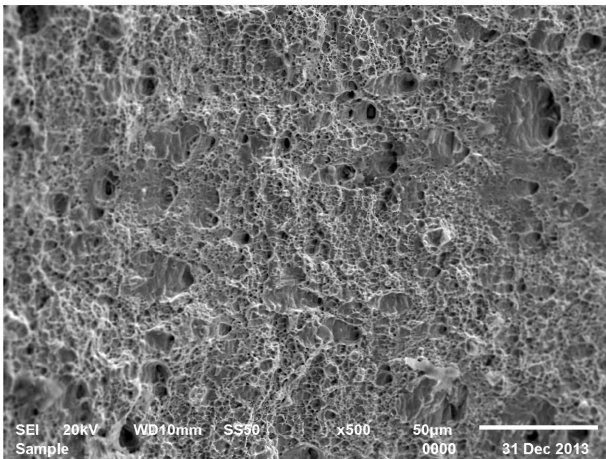
Fracture behaviour similar to that of the room temperature test was observed in the parent metal and weld joint tested at 600 °C. The fracture occurred at the parent metal in case of both the joints tested 600 °C. The dimples are much finer in room temperature test than the test at 600 °C which is evidenced by the high percentage of elongation observed in the room temperature test of both parent metal and weld joint. The fracture surface of parent metal and weld joint tested at both condition invariably consists of dimples of varying sizes

evidencing ductile mode of failure, with voids which are attributed to the precipitates, these precipitates act as crack initiation sites for the failure.

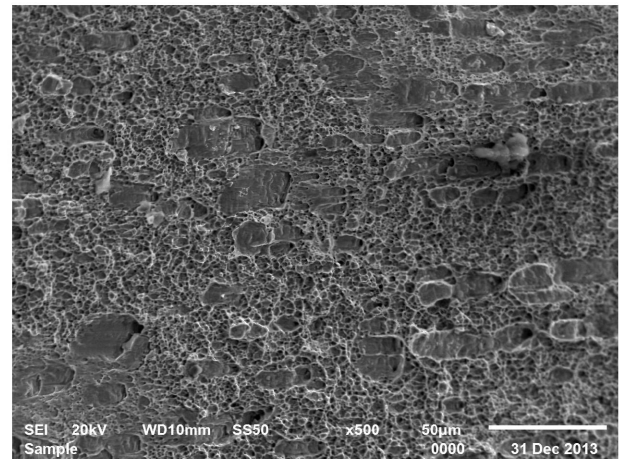
4.0 DISCUSSION

The fully austenitic type of solidification (A-Type) had resulted in weld metal which is fully austenitic, with no delta ferrite (refer Fig. 3a). The boundaries are decorated by (Nb, Mo) (C, N) precipitates which are attributed to the higher amount of Nb and Mo addition to the filler metal [8-11]. In primary austenite type of solidification, Nb and Mo being ferrite formers tend to segregate along the grain boundaries and form carbides along the grain boundaries. The high carbon content in AISI 304HCu is hence stabilized by the addition of carbide forming elements Nb and Mo to the filler metal. The presence of thermally stable microstructure in AISI 304HCu which forms the HAZ region of the weld joint does not allow the softening of material due to grain coarsening [9-11].

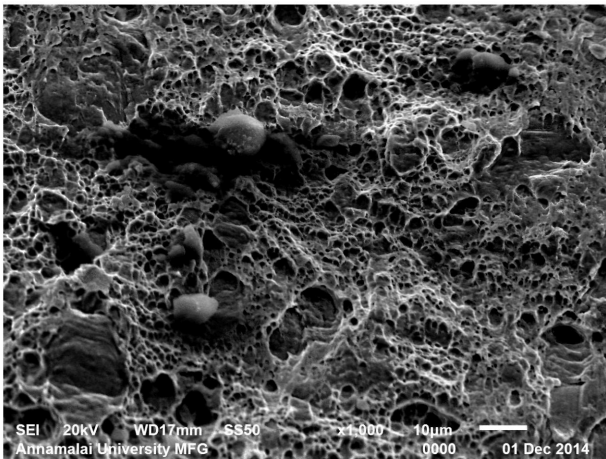
Tensile test results revealed that the tensile strength of the weld joint at all test temperature is higher than that of parent metal strength values. However the tensile strength and elongation values decrease with increase in test temperature, which is attributed to the dislocation annihilation at higher temperatures [12]. The increase in strength of the weld joint is attributed to the presence of weld metal with higher hardness and finer subgrain boundaries than the parent metal in the weld joint [13,14]. The higher hardness in the weld metal was achieved by the addition of Nb and Mo in the filler metal which forms carbides within and along the grain boundaries, and there by increasing the hardenability of the weld metal. The dislocations which are which set free during tensile loading are hindered by the (Nb,Mo) (C,N) precipitates in the weld metal offers greater resistance to deformation.



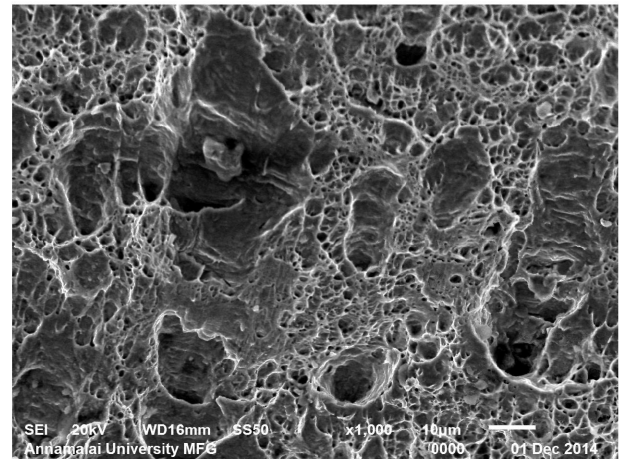
a) Parent metal tested at RT



b) Weld joint tested at RT (failure at PM)



c) Parent metal tested at 600 °C



d) Weld joint tested at 600 °C (failure at PM)

Fig. 6 : Fracture surface of parent metal and weld joint

5.0 CONCLUSIONS

1. AISI 304HCu welded with filler addition using GTAW process resulted in fully austenitic weld metal without delta ferrite. The weld joint with no delta ferrite is suitable for high temperature application as the risk of transformation of delta ferrite to sigma phase can be avoided.
2. The addition of filler with increased Nb and Mo content to the weld metal of AISI 304HCu GTAW joint resulted in joints with tensile strength higher than the parent metal at all test temperatures. Hence AISI 304HCu welded with increased Mo and Nb filler addition can be effectively applied to the fabrication of ultra super critical boiler tubes.

3. The tensile strength of both parent metal and weld joint are sensitive to the test temperature, as the tensile strength and elongation decreases with increase in test temperature.

ACKNOWLEDGEMENTS

The authors wish to express their sincere thanks to M/s Mailam India Ltd, Pondicherry, India for providing financial assistance to carry out this research work through the Mailam India Research (MIR) Fellowship, M/s Salzgitter Mannesmann Stainless Tubes Italia Srl of Italy for supplying the AISI 304HCu tubes required to carry out this work, and The Director, Naval Materials Research Laboratory (NMRL), Ambernath, Mumbai for providing the facility to carry out hot tensile testing.

REFERENCES

1. Viswanathan, R. and Bakker, W.T. (2000); Materials for Ultra Supercritical Fossil Power Plants, EPRI Technical report TR-114750.
2. Singh, K. (2006); Advances in materials for advanced steam cycle power plants, BHEL.J., 27, pp. 1-19.
3. Chi, C., Yu H. and Xie, X. Advanced austenitic stainless steel for ultra-supercritical (USC) fossil power plants, University of Science and Technology, Beijing, China.
4. Vinoth Kumar, M. and Balasubramanian, V. (2014); Effect of autogenous GTAW welding processes on tensile properties of super 304H austenitic stainless steel joints, Proc. IIW Int. Cong. IC-2014, New Delhi, India.
5. Sen, I., Amankwah, E., Kumar, N.S., Fleury, E., Ohishi, K., Hono, K. and Ramamurty, U. (2011); Microstructure and mechanical properties of annealed SUS 304H austenitic stainless steel with copper, J Mater. Sci. Eng. A, 528, pp. 4491-4499.
6. Ha, V.T., and Jung, W.S., (2012); Creep behavior and microstructure evolution at 750°C in a new precipitation strengthened heat-resistant austenitic stainless steel, J Mater. Sci. Eng. A, 558, pp. 103-111.
7. Yang, H., Peng, F., Miao, X. and Yang, X. (2006); Investigation of the aging behavior on boiler steel tube super304H, J. Press. Equip. Sys., 4, pp. 96-99.
8. Kou, S. (2003), Welding Metallurgy, John Wiley & Sons Publication.
9. Shankar, V., Gill, T. P. S., Mannan, S. L. and Sundaresan, S. (2003); Solidification cracking in austenitic stainless steel welds, Sadhana, 28, pp. 359-382.
10. Lippold, J. C. and Savage, W. F. (1979); Solidification of Austenitic Stainless Steel Weldments : Part2 - The Effect of Alloy Composition on Ferrite Morphology, Proc. of AWS 60th Annual Meeting held in Detroit, Michigan.
11. Bhadeshia, H.K.D.H., David, S.A. and Vitek, J.M. (1991); Solidification sequences in stainless steel dissimilar alloy welds, J. Mater. Sci. Technol., 7, pp.50-61.
12. Choudhary B.K. and Rao Palaparti D.P. (2012); Comparative tensile flow and work hardening behaviour of thin section and forged thick section 9Cr-1Mo ferritic steel in the framework of Voce equation and Kocks-Mecking approach, J. Nucl. Mater., 430, pp. 72-81.
13. Wang, S.Q., Liu, J.H. and Chen D.L. (2014); Effect of strain rate and temperature on strain hardening behavior of a dissimilar joint between Ti-6Al-4V and Ti17 alloys, J. Mater. Des., Vol. 56, pp. 174-184.
14. Fan, Z., Mingzhi H. and Deke, S. (1989); The relationship between the strain-hardening exponent n and the microstructure of metals, J. Mater. Sci. Eng, A122, pp. 211-213.